Int. J. Electron. Commun. (AEÜ) 84 (2018) 162–170

Contents lists available at ScienceDirect

Int. J. Electron. Commun. (AEÜ)

journal homepage: www.elsevier.com/locate/aeue

Regular paper

gold-MUSIC based DOA estimation using ULA antenna of DS-CDMA sources with propagation delay diversity

Amiya Dey, Arnab Nandi*, Banani Basu

Electronics and Communication Engineering Department, National Institute of Technology Silchar, Silchar 788010, Assam, India

ARTICLE INFO

Keywords:
DS-CDMA
Gold code
Near-Far effect
ULA
DOA
gold-MUSIC

ABSTRACT

Direction of Arrival (DOA) estimation using *gold*-MUSIC is achieved for Uniform Linear Array (ULA) antenna based Direct-Sequence Code Division Multiple Access (DS-CDMA) sources having different Propagation Delay. The DOA is estimated by different MUSIC (Multiple Signal Classification) algorithms for M signal sources with Phase Shift Keying (PSK) transmission in presence of Additive White Gaussian Noise (AWGN). Spatial spectrum, computational efficiency and Root Mean Square Error (RMSE) of DOA estimation using *gold*-MUSIC over MUSIC and Root-MUSIC algorithms are studied meticulously. The effects of number of ULA elements, Data length and arrival angle on RMSE of DOA are also conferred here.

1. Introduction

Direct-Sequence Code Division Multiple Access (DS-CDMA) technology is deployed in the air interface as the backbone of third generation (3G) wireless systems [1–3]. The demand for improved adaptive antenna array DS-CDMA system performance is increasing because of its advantageous implementation and security related applications. Multiple Access (MA) allows efficient use of wireless bandwidth. Spread-spectrum communication achieves excellent potential of large bandwidth and very low forward error control coding [4].

Coherence detection requires exact channel estimation [5]. Antenna arrays at base station of Multicarrier (MC) DS-CDMA system enable estimation of space-time and channel parameters with user locations [6–8]. Receiver antenna arrays detect the information by suppressing interference, exploiting Pseudo Noise (PN) code, users spatial separation and space-time processing [9,10].

In practice, proper Direction of Arrival (DOA) estimation by Multiple Signal Classification (MUSIC), Estimation of Signal Parameters via Rotational Invariance Techniques (ESPRIT), etc. algorithms require more number of array elements than the number of active users [9,11]. DOA estimator with code-matched filters and parallel MUSIC models the interference from other users as Gaussian noise [12]. As the spatial spectrum interval goes coarser, MUSIC gives less accurate results [13]. Root-MUSIC can be applied only to Uniform Linear Array (ULA) antenna for improving accuracy with no dependency on spatial spectrum interval [13]. *gold*-MUSIC employed with any antenna array geometry provides more accurate results, less complexity and computational advantage than MUSIC and Root-MUSIC [13].

gold-Section Univariate (GSU) method provides excellent results with lower number of iterations, smaller number of snapshots and lower Signal to Noise Ratio (SNR) [13]. *gold*-MUSIC offers improved Root Mean Square Error (RMSE), resolution, complexity, SNR sensitivity and calibration sensitivity of estimated DOA as compared to Delay and Sum (DAS), Max entropy, Capon, MUSIC, Root MUSIC and ESPRIT techniques [14,15]. Generalised (G)-MUSIC, Matching Pursuit (MP)-MUSIC, $\ell_{1,2}$-MUSIC and M$\ell_{1,2}$-MUSIC are joint approaches of Compressive Sensing (CS) and MUSIC for DOA estimation in presence of multipath [16]. *gold*-MUSIC can further enhance estimation performance of combined CS and MUSIC approaches.

Sparse aperodic arrays accomplish any design by utilizing least possible active array elements with enough degrees of freedom in that task [17]. *gold*-MUSIC can be applied for DOA estimation by sparse aperiodic antenna arrays following similar procedure of working with ULA. Mapping of source covariance matrix for sparse aperiodic arrays to ULA of same aperture facilitates desired outcome [18]. *gold*-MUSIC DOA estimate using sparse aperiodic arrays designed by CS approach can offer subsequent deterministic and probabilistic advantages [17].

This paper assesses ULA based DOA estimation of DS-CDMA sources employing *gold*-MUSIC. The Propagation Delay diversity in presence of Additive White Gaussian Noise (AWGN) and Near-Far effect are also incorporated in the system model. The DOA is estimated for signal sources with Phase Shift Keying (PSK) transmission in non-overlapping time frame. The GSU method used here is applied to the objective function itself for obtaining the ceiling. It is easy to implement, facilitated by Golden Ratio with very small number of iterations. In this article, fast realization of DOA values is achieved with single scan and

* Corresponding author.
E-mail addresses: amiyo4u@gmail.com (A. Dey), nandi_arnab@ieee.org (A. Nandi), basu_banani@ieee.org (B. Basu).

https://doi.org/10.1016/j.aeue.2017.11.029
Received 24 July 2017; Accepted 28 November 2017

very low complexity. Spatial spectrum, RMSE and computational complexity of DOA estimate by *gold*-MUSIC compared to Root MUSIC and MUSIC are detailed here. The impact of different Data length, number of ULA elements and arrival angle on RMSE of DOA are also studied for different MUSIC algorithms.

2. ULA antenna based DS-CDMA

The data security associated with spread spectrum technology escalates the interest in Direct Sequence Spread Spectrum (DSSS) communication. The Near-Far effect is experienced by the DS-CDMA receiver due to variations in power received. Due to efficient bandwidth and power utilization property, the DSSS system is suitable for operating in Near-Far environment. In DS-CDMA, multiple users share the whole channel bandwidth and are multiplexed by PN codes [3,5,19,20].

The DS-CDMA signal for m^{th} user passing through the transmission medium is [7,21,22],

$$s_{DS_m}(t) = g_m\sqrt{P_m}\,d_{k_s}^{(m)}c_{G_m}(t) \tag{1}$$

The sampling instant is $t = k_sT_s$, where the sampling interval is T_s and k_s is an integer. The chip duration is $T_c = T_s/L_c$, where L_c is Spreading Factor. The PSK transmitted data in single T_s for m^{th} user is $d_{k_s}^{(m)}$. The m^{th} user signal strength is $g_m\sqrt{P_m}$. The m^{th} user scalar gain for channel is g_m. The transmission power for m^{th} user is P_m. $c_{G_m}(t)$ is the Gold code sequence operating as the PN code for m^{th} user. The DS-CDMA signal in Near-Far effect for m^{th} user can be deduced from Eq. (1) as,

$$s_{DSnf_m}(t) = g_m\sqrt{P_{nf_m}}\,d_{k_s}^{(m)}c_{G_m}(t) \tag{2}$$

where the Near-Far power received for m^{th} user is P_{nf_m}.

The channel spatial aspect, i.e., incoming signal DOA is exploited by utilizing beamforming techniques for tracking and separating signals [23–25]. Array antennas improve the performance of DS-CDMA systems by reducing Multiple Access Interference (MAI) [26–29]. Suppose, E_b is Energy per bit and $N_0/2$ is AWGN Power Spectral Density (PSD). Then, SNR is $2E_b/N_0$ and noise variance for single antenna receiver is [28],

$$\sigma_N^2 = \frac{N_0}{2} \tag{3}$$

Let, N is the number of omnidirectional antenna elements. In receiver consisting of antenna array, the noise power is reduced by N times as compared to that of single antenna receiver. So, the noise variance of receiver consisting of antenna array becomes [28],

$$\overline{\sigma}_N^2 = \frac{\sigma_N^2}{N} = \frac{\frac{N_0}{2}}{N} \tag{4}$$

In general, when the DS-CDMA signals impinge on the ULA system of N elements from M signal sources in Near-Far environment, the received signal by n^{th} array element is [30–33],

$$x_n(t) = \sum_{m=1}^{M} s_{DSnf_m}(t)e^{-j2\pi\frac{d_n}{\lambda}\sin\theta_m} + n_n(t) \tag{5}$$

where d_n is the distance between n^{th} and reference antenna array element. θ_m is the DOA of the m^{th} signal source. λ is the carrier signal wavelength of signal sources and $n_n(t)$ is the additive noise.

Let the ULA elements have half wavelength inter-element spacing. Then the received signal by the ULA can be enumerated as [14,32],

$$\mathbf{x}(t) = \mathbf{A}\mathbf{s}(t) + \mathbf{n}(t) \tag{6a}$$

$\mathbf{x}(t)$ is $N \times 1$ vector given as,

$$\mathbf{x}(t) = [x_1(t)x_2(t)x_3(t)\ldots x_N(t)]^T \tag{6b}$$

$\mathbf{s}(t)$ is $M \times 1$ vector given as,

$$\mathbf{s}(t) = \left[s_{DSnf_1}(t)s_{DSnf_2}(t)s_{DSnf_3}(t)\ldots s_{DSnf_M}(t)\right]^T \tag{6c}$$

$\mathbf{n}(t)$ is $N \times 1$ vector given as,

$$\mathbf{n}(t) = [n_1(t)n_2(t)n_3(t)\ldots n_N(t)]^T \tag{6d}$$

The array factor $\mathbf{A}$ is an $N \times M$ matrix, whose m^{th} column is given as,

$$\mathbf{a}(\theta_m) = \left[1e^{-j\pi\sin\theta_m}e^{-j2\pi\sin\theta_m}\ldots e^{-j(N-1)\pi\sin\theta_m}\right]^T \tag{6e}$$

When the signals impinging on ULA have same delay, then, at any instant, the received signal by n^{th} array element follows Eq. (5). When signals impinging on ULA have different delay, so that, they can occur in non-overlapping time frame, then, at any instant, the n^{th} array element gets the signal from single signal source. Thus, received signal has no MAI effect and is given as,

$$x_{0n}(t) = s_{DSnf_0}(t)e^{-j2\pi\frac{d_n}{\lambda}\sin\theta_0} + n_{0n}(t) \tag{7}$$

where $s_{DSnf_0}(t)$ is the DS-CDMA signal transmitted by the signal source with DOA of θ_0 and $n_{0n}(t)$ is the additive noise.

3. DOA estimation using *gold*-MUSIC

The DOA estimated by MUSIC algorithm gives sharp peak at arriving angle with minimized magnitude at other angles [13]. The received signal by ULA in Eq. (7) is taken as the input of this estimator. The DS-CDMA Data length is given as,

$$L_t = L_dL_c \tag{8}$$

where L_d is the actual Data length.

The input covariance matrix is calculated as,

$$\mathbf{R}_{xx} = \frac{1}{L_t}\sum_{l=1}^{L_t} x_{0n}(t_l)x_{0n}^H(t_l) \tag{9}$$

Eigenvalue decomposition on the covariance matrix gives the eigenvectors $\mathbf{E_N}$. The DOA of DS-CDMA user by MUSIC is provided by the objective function as [15],

$$P(\theta) = \frac{1}{\mathbf{a}^H(\theta)\mathbf{E_N}\mathbf{E_N}^H\mathbf{a}(\theta)} \tag{10}$$

where θ is the scanning angle.

The polynomial of $\mathbf{E_N}$ is solved in Root-MUSIC DOA estimation. GSU minimization applied on the coarse of $P(\theta)$ avails the arrival angles in *gold*-MUSIC [13].

GSU locates the extreme of a univariate function by consecutively reducing the range within which extreme is supposed to occur. Let the coarse interval is θ_a to θ_b with $\theta_a < \theta_b$ in the DOA interval of -90° to 90°. The intermediate points θ_c and θ_d are chosen as [34],

$$\theta_c = \theta_a + g(\theta_b - \theta_a) \tag{11a}$$

$$\theta_d = \theta_b - g(\theta_b - \theta_a) \tag{11b}$$

where the Golden Ratio is given as,

$$g = (\sqrt{5}-1)/2 \tag{11c}$$

$P(\theta)$ is evaluated at θ_a, θ_b, θ_c and θ_d. If $P(\theta_d) > P(\theta_c)$, then $\theta_b = \theta_c$ and $\theta_c = \theta_d$, else $\theta_a = \theta_d$ and $\theta_d = \theta_c$ in the next iteration. Moderate number of iterations can provide DOA value accurately.

The RMSE of DOA estimate is calculated by [15],

$$\text{RMSE} = \sqrt{\frac{1}{R_t}\sum_{e=1}^{R_t}(\theta_e - \theta_0)^2} \tag{12}$$

where θ_e is the estimated DOA for e^{th} snapshot, θ_0 is the real DOA and R_t is number of runtimes.

The time complexity of DOA estimation algorithms are given as [13,35,36]. C_M is the coarse scanning angle for MUSIC. Table 1 explains

Table 1
Time complexity of algorithms.

Algorithm	Complexity
MUSIC	$O(L_dN^2 + N^3) + O(MN^2 \times 180/C_M)$
Root MUSIC	$O(L_dN^2 + N^3) + O((N - M)\, N^3)$
gold-MUSIC	$O(L_dN^2 + N^3) + O(MN^2)$

Table 2
Common system parameters for Case 1 and Case 2.

System parameters	Description
No. of users or signal sources (M)	4
Digital carrier modulation	QPSK
Spreading factor (L_c)	31
PN code	Gold sequence (31 × 4)
Near-Far environment	User 1 is 5.9 dB and User 3 is 4.1 dB higher than other 2 users
SNR	20 dB
No. of users taken at a time for analysis (N_s)	1
Noise dimension	$N \times (L_d * L_c)$

Table 3
Additional system parameters for Case 1.

System parameters	Description
No. of antenna elements (N)	4 or 5 or 6
Actual DOA (θ_1) (same for all users)	45°
Actual data length (L_d)	2000
Propagation delay	0, T_t, $2T_t$, $3T_t$

that the complexity of MUSIC is much higher than other two algorithms. It is clear that *gold*-MUSIC has less complexity than Root MUSIC. MUSIC algorithms complexity increases with increase in Data length, ULA elements and users. Significantly, C_M majorly contributes toward high complexity of MUSIC.

4. System design and implementation

The spreading of data bits of DS-CDMA users is performed using Gold code with M-ary PSK modulation. The DS-CDMA signals transmitted by M users are added with AWGN in the propagation channel. The noise is represented by random variables with some standard deviation occurring for the dimension that is dependent on ULA elements, Spreading Factor and Data length. The design, implementation and performance analysis are assessed in MATLAB® platform.

4.1. Algorithm of ULA based DOA estimation using MUSIC algorithms for DS-CDMA system in AWGN channel with Near-Far effect

Step 1: Number of users M, actual Data length L_d and Spreading Factor L_c are specified.
Step 2: The $L_c \times 1$ Gold code $c_{G_m}(t)$ is generated as the PN sequence for each of the M users concerned.
Step 3: The PN codes are made effective to the level of the Near-Far power P_{nf_m} associated with different users.
Step 4: The real DOA θ_m is declared for all users.
Step 5: The number of ULA elements N is specified and array factor $\mathbf{a}(\theta_m)$ is calculated for all users.
Step 6: The PSK modulation symbols $d_{k_s}^{(m)}$ are generated using the combination of L_d and M for different signal phases.
Step 7: Using effective Gold code and $d_{k_s}^{(m)}$, the DS-CDMA signal $s_{DSnf_m}(t)$ is formed for all users.
Step 8: The DS-CDMA signal associated with every user $s_{DSnf_m}(t)$ is transmitted along the AWGN channel $\mathbf{n}(t)$ formed with desired L_c, SNR and standard deviation S_d using randomly generated variables of $N \times L_d * L_c$ dimension.
Step 9: ULA antenna receives single DS-CDMA user signal $s_{DSnf_0}(t)$ and its output is obtained as $x_{0n}(t)$ with added noise.
Step 10: $x_{0n}(t)$ is used by the DOA estimation algorithms for calculating the input covariance matrix.
Step 11: The eigenvalue decomposition on covariance matrix gives eigenvectors.
Step 12: The DOA is estimated using MUSIC, Root MUSIC and *gold*-MUSIC algorithms separately.
Step 13: The RMSE of DOA estimation algorithms are calculated from the difference of estimated DOA θ_e and real DOA θ_0.

5. Results and performance analysis

Here, three diverse scenarios are considered for users having different Propagation Delay – i. four users with equal DOA, ii. four users with different DOA, iii. three users with different DOA. Let data transmission duration for each user is T_t.

User 1 and User 3 are stronger and near users. User 2 and User 4 are weaker and far users for Case 1 and Case 2. User 2 is the weaker and far user for Case 3. Table 2 shows the common system parameters involved in Case 1 and Case 2. Four users are operated with Quadriphase-Shift Keying (QPSK) transmission in presence of Near-Far effect and AWGN. Users operation in non-overlapping time formulates the number of users at any instant as one.

5.1. Case 1

This case considers signal sources with equal DOA and different Propagation Delay. The additional system parameters used in this case are given in Table 3. The DS-CDMA system is operated with users having same DOA of 45° for different number of ULA elements. The Propagation Delay of users is chosen to satisfy their operation in non-overlapping time frame.

Table 4 illustrates about negligible deviation of estimated DOA from the actual DOA at 20 dB SNR with varying ULA elements for different DOA estimation algorithms and DS-CDMA users. The estimated DOA improves with increasing number of ULA elements. Also, the DOA estimate by *gold*-MUSIC is superior to other algorithms.

Table 4
Measurement of equal DOA of signal sources with different Propagation Delay.

User	Measured DOA (Degrees)								
	4 element ULA			5 element ULA			6 element ULA		
	MUSIC	Root MUSIC	*gold*-MUSIC	MUSIC	Root MUSIC	*gold*-MUSIC	MUSIC	Root MUSIC	*gold*-MUSIC
User 1	45.0249	45.0209	45.0142	44.9874	44.9394	44.9999	44.9381	44.9689	44.9999
User 2	44.8979	44.9394	44.9999	44.9894	44.9984	44.9994	44.9954	44.9989	44.9998
User 3	45.0239	45.0139	45.0101	44.9893	44.9897	44.9949	44.9921	44.9989	44.9999
User 4	44.9179	44.9596	44.9797	44.9374	44.9631	44.9899	44.9635	44.9872	44.9998

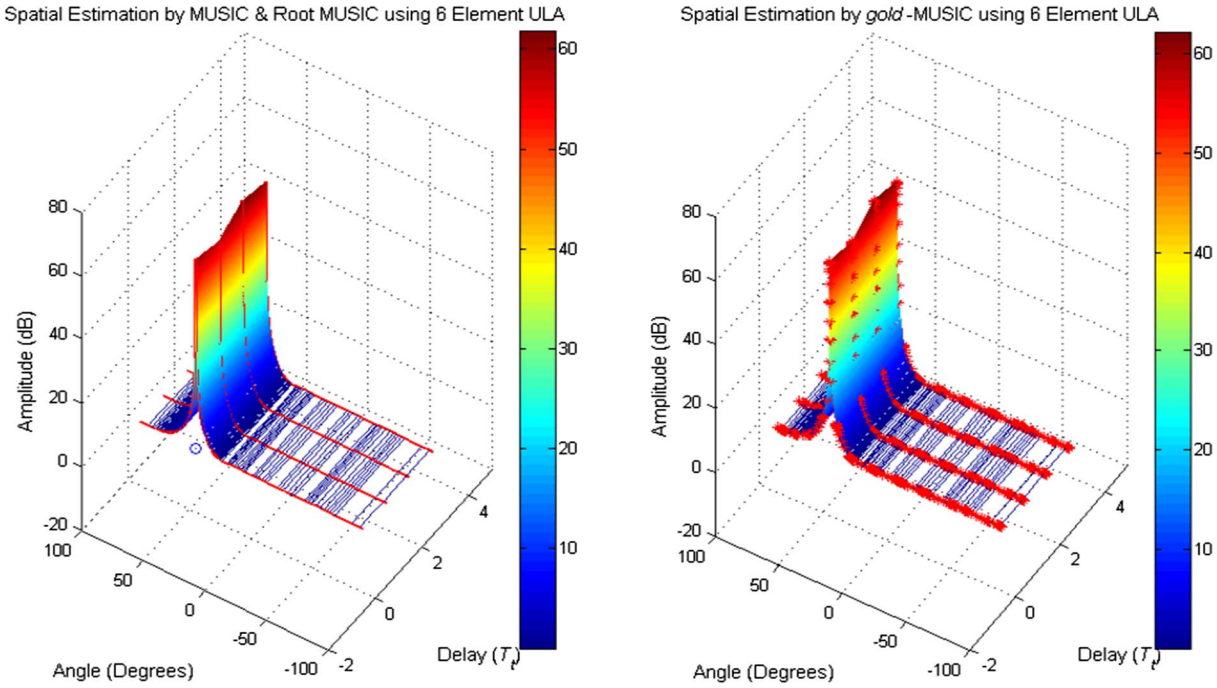

Fig. 1. Multisource (equal DOA and different Propagation Delay) Spatial Estimation by MUSIC, Root MUSIC and *gold*-MUSIC using 6 element ULA.

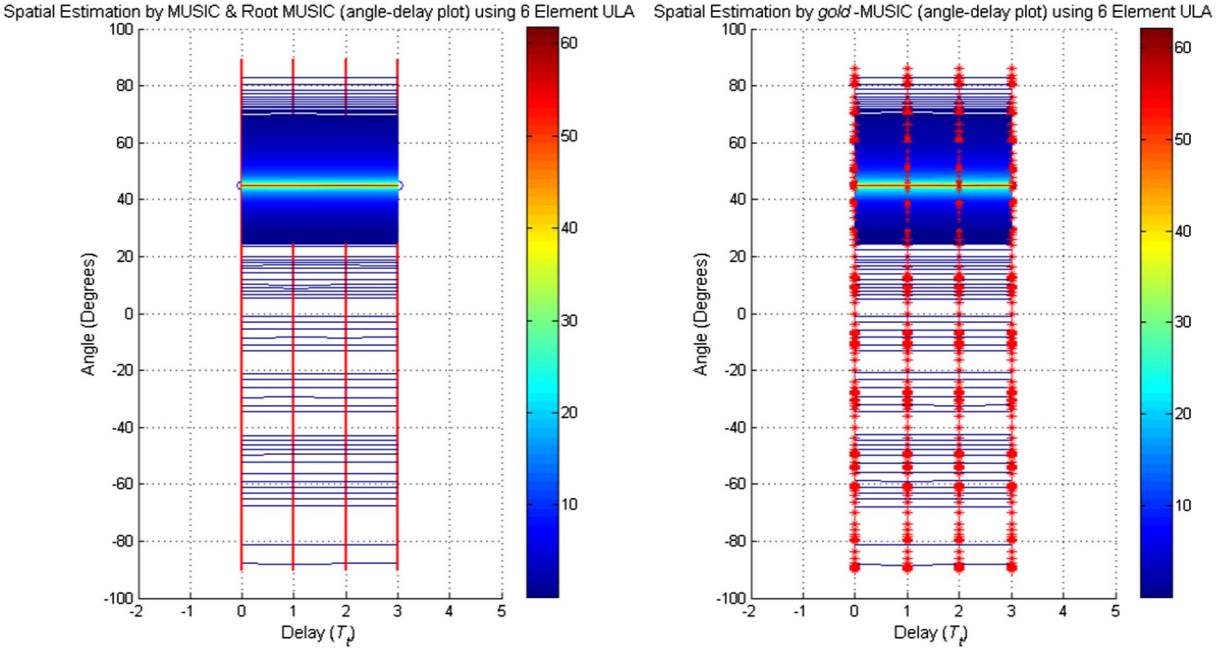

Fig. 2. Multisource (equal DOA and different Propagation Delay) Spatial Estimation (angle-delay plot) by MUSIC, Root MUSIC and *gold*-MUSIC using 6 element ULA.

Table 5
Additional system parameters for Case 2.

System parameters	Description
No. of antenna elements (N)	2 or 3 or 4
Actual DOA (θ_1, θ_2, θ_3, θ_4)	10°, 70°, −5°, 50°
Actual data length (L_d)	2400
Propagation delay	0, T_b, $2T_b$, $3T_t$

The plots in Fig. 1 show the amplitude, angle and delay behavior of spatial MUSIC and *gold*-MUSIC spectrum using 6 element ULA for DS-CDMA users in Case 1. The spatial spectrums have sharp spikes nearly at the angle of arrival of 45° for all the users with respective delays. Spatial spectrums peak is about 60 dB and gradually decrease in both sides of DOA along the angle axis retaining almost flat sidelobes. Root MUSIC shows only circled point as DOA.

The plots in Fig. 2 evaluate corresponding amplitude variation in angle-delay surface. The plots show uniform level of amplitude variation along delay axis since all users have same DOA. DOA spikes

Table 6
Measurement of different DOA of signal sources with different Propagation Delay.

User	Measured DOA (Degrees)								
	2 element ULA			3 element ULA			4 element ULA		
	MUSIC	Root MUSIC	*gold*-MUSIC	MUSIC	Root MUSIC	*gold*-MUSIC	MUSIC	Root MUSIC	*gold*-MUSIC
User 1	9.9827	9.9877	9.9897	10.0162	10.0112	10.0067	9.9925	9.9965	9.9999
User 2	70.0681	70.0371	70.0183	70.0147	70.0091	70.0041	70.0087	70.0045	70.0005
User 3	−5.0196	−5.0106	−5.0036	−4.9961	−4.9981	−4.9991	−5.0024	−5.0011	−5.0007
User 4	49.9765	49.9885	49.9965	50.0229	50.0136	50.0022	49.9903	49.9953	49.9999

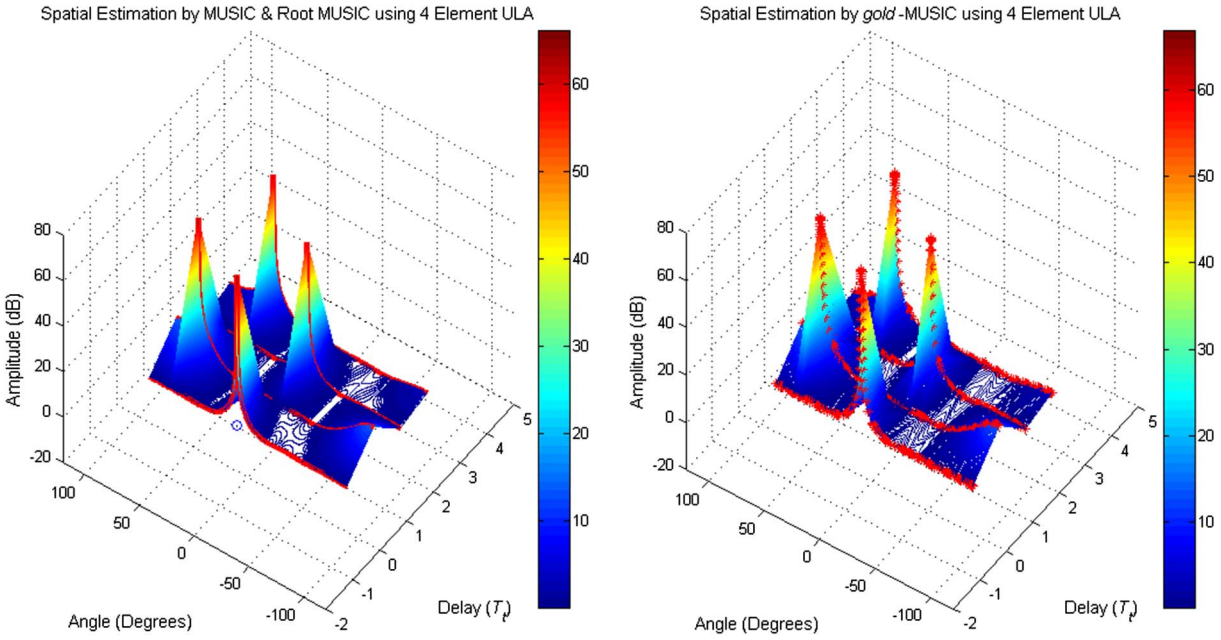

Fig. 3. Multisource (different DOA and different Propagation Delay) Spatial Estimation by MUSIC, Root MUSIC and *gold*-MUSIC using 4 element ULA.

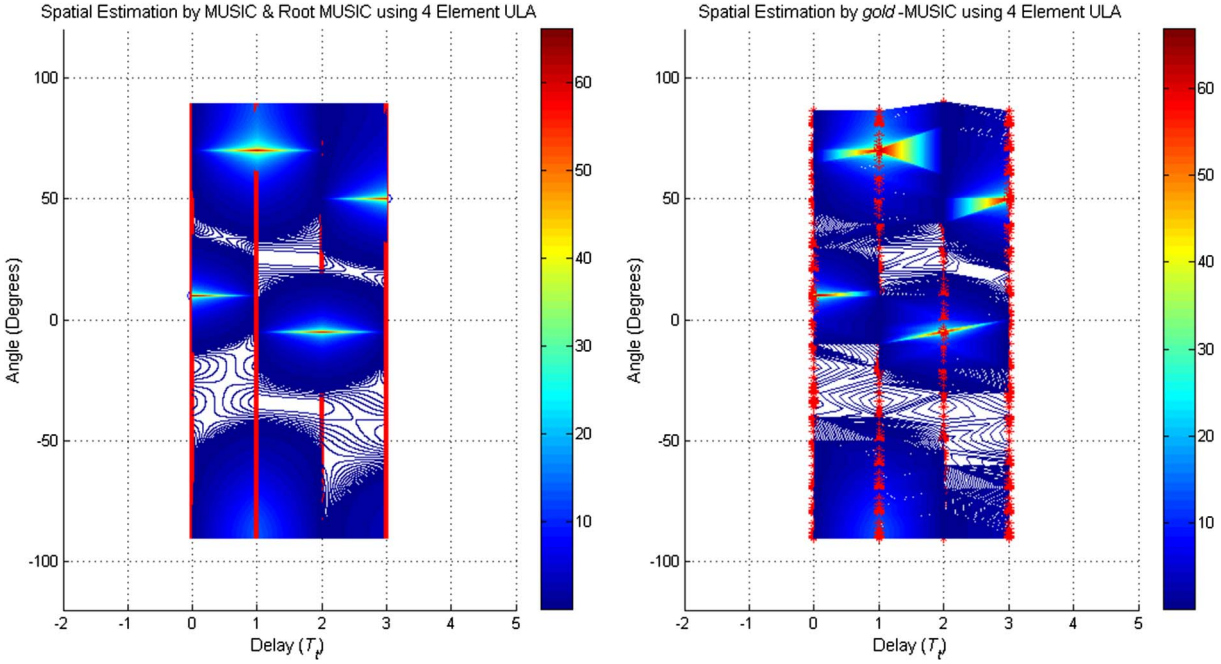

Fig. 4. Multisource (different DOA and different Propagation Delay) Spatial Estimation (angle-delay plot) by MUSIC, Root MUSIC and *gold*-MUSIC using 4 element ULA.

Table 7
System parameters for Case 3.

System parameters	Description
No. of users or signal sources (M)	3
Digital carrier modulation	4-ary PSK
Spreading factor (L_c)	31
PN code	Gold sequence (31 × 3)
Near-Far environment	User 1 is 5.9 dB and User 3 is 4.1 dB higher than other user
No. of antenna elements (N)	2 or 3 or 4 (for Figs. 5–7); 2–16 (for Fig. 8)
SNR	0 dB to 20 dB (for Figs. 5–7) 15 dB (for Fig. 8)
MUSIC RMSE run times	100
Antenna inter-element distance (d)	$\lambda/2$
No. of users taken at a time for analysis (N_s)	1
Actual DOA (θ_1, θ_2, θ_3)	20°, −45°, 75° (for Figs. 5–7) 30°, −25°, 55° (for Fig. 8)
Actual data length (L_d)	15,000 (for Figs. 5 and 6) 2000, 5000 and 10,000 (for Fig. 7) 200, 1000 and 1800 (for Fig. 8)
Noise dimension	$N \times (L_d * L_c)$
Propagation delay	0, T_t, $2T_t$

vicinity is very small. *gold*-MUSIC uses very less number of coarse points of objective function, facilitated by Golden Ratio to achieve the desired estimate.

5.2. Case 2

This case considers signal sources having different DOA and different Propagation Delay. The additional system parameters for this case are specified in Table 5. The DS-CDMA users having different DOA are operated with different ULA elements. Propagation Delay of users is occurring in non-overlapping time frame.

Table 6 depicts very minor variation of estimated DOA from the actual DOA for different ULA elements, Spatial Estimation algorithms and DS-CDMA users. DOA estimation improves with increment in number of ULA elements at SNR of 20 dB. Moreover, *gold*-MUSIC provides superior DOA estimate than others.

Fig. 3 clarifies the amplitude, angle and delay behavior of spatial MUSIC and *gold*-MUSIC spectrum using 4 element ULA in Case 2. The DOA spatial spectrums have distinguishable spikes almost at the arrival angles 10°, 70°, −5° and 50° for all the 4 users. The spatial spectrums amplitude is about 65 dB with nearly flat sidelobes. Lesser number of coarse points is taken by *gold*-MUSIC in obtaining required estimate. Circled point is provided as DOA by Root MUSIC.

Fig. 4 assesses corresponding equivalent amplitude variation in angle-delay surface. Plots show different deviation of amplitude levels along delay and angle axis for any particular user. Gradual decrement of spatial spectrum occurs around small vicinity of DOA spikes along both the axis.

5.3. Case 3

This case considers 3 DS-CDMA signal sources with different DOA and different Propagation Delay. The RMSE of DOA estimation is analyzed following system parameters in Table 7. Here, three users are operated with 4-ary PSK transmission in AWGN and Near-Far effect. Number of users operating at any instant is taken as one to satisfy their non-overlapping time usage. SNR is taken as 15 dB for complexity analysis and varied from 0 dB to 20 dB for RMSE analysis. Better estimate of RMSE is obtained by choosing high experimental run times. Different DOA, Propagation Delay, Data length and ULA elements are chosen to facilitate diversity in analysis.

Fig. 5 shows decreasing RMSE of the DOA estimate with increasing ULA elements. *gold*-MUSIC is providing superior RMSE than MUSIC and Root MUSIC with increasing SNR for 20° DOA. Fig. 6 demonstrates decreasing RMSE with decreasing value of arrival angle. *gold*-MUSIC avails improved RMSE performance than other algorithms using 4 element ULA.

Higher value of ULA elements and lower DOA value can provide even lower RMSE. The RMSE of DOA estimation decreases with increase in DS-CDMA transmission Data length as coined from Fig. 7. RMSE of *gold*-MUSIC is better than other MUSIC algorithms for 75° DOA, $N = 3$ and different Data length. Higher Data length can deliver even lower RMSE.

Fig. 8 shows the variation of RMSE with the Order of Complexity of DOA estimation algorithms for different Data length of User 1 with increasing ULA elements. As the ULA elements and Data length

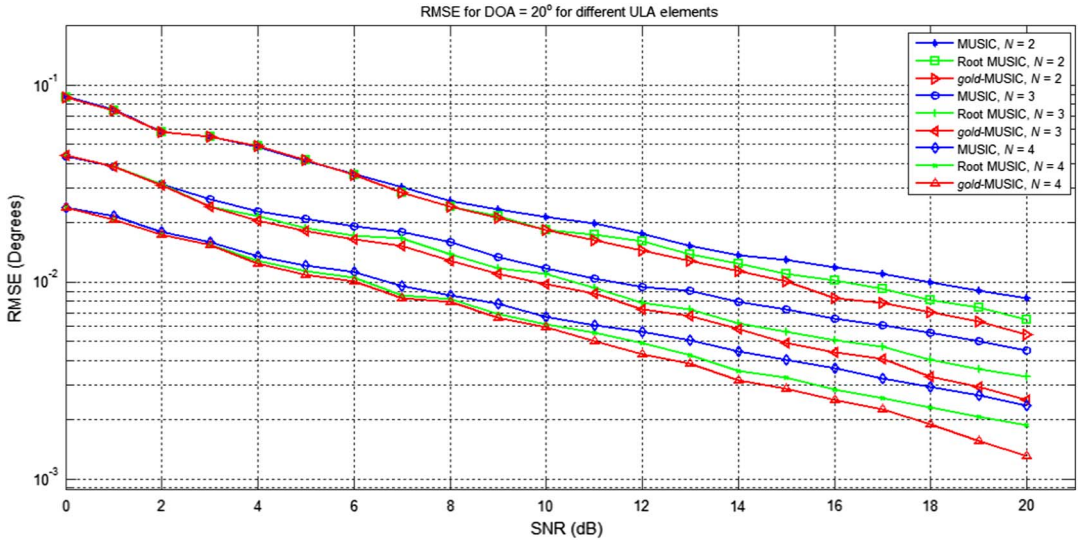

Fig. 5. RMSE of estimation for DOA of 20° using different ULA elements for MUSIC, Root MUSIC and *gold*-MUSIC.

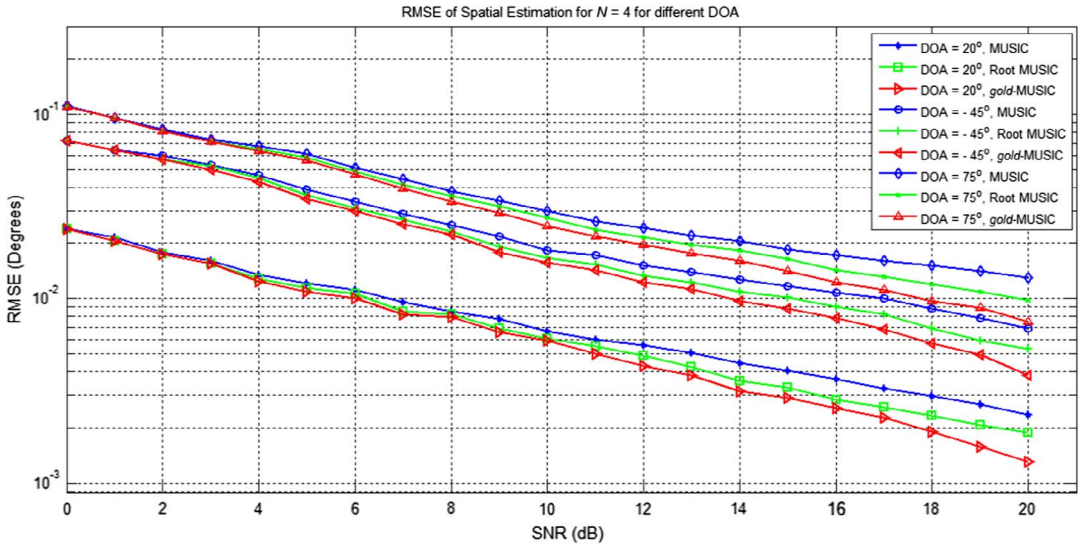

Fig. 6. RMSE of DOA Estimation using 4 element ULA for different arrival angles by MUSIC, Root MUSIC and *gold*-MUSIC.

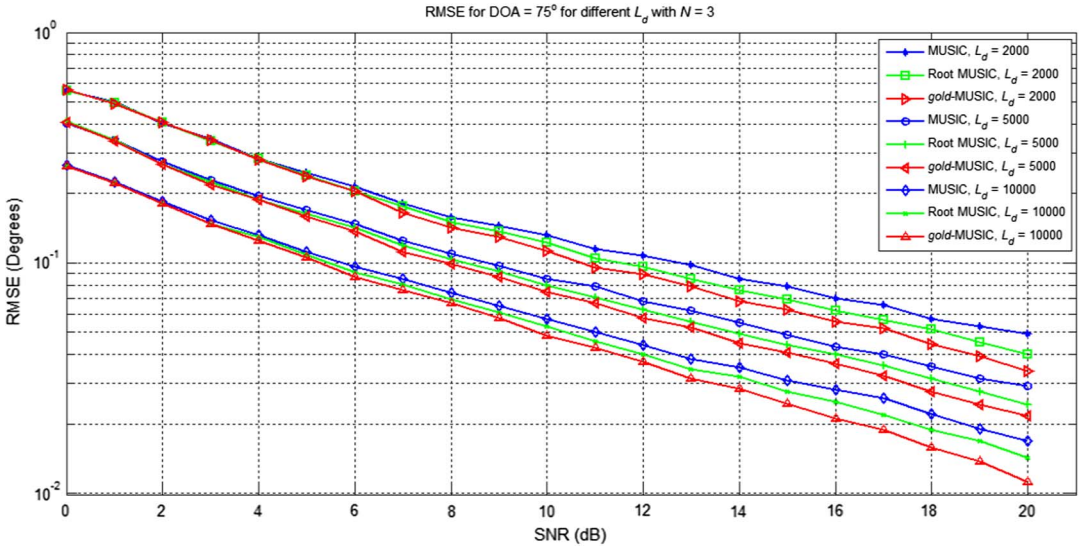

Fig. 7. RMSE of estimation for DOA of 75° using 3 element ULA for different Data length by MUSIC, Root MUSIC and *gold*-MUSIC.

increase, complexity increases and RMSE decreases. Beyond certain Order of Complexity, the RMSE value attains a floor around 10^{-2} for MUSIC and 10^{-3} for Root MUSIC and *gold*-MUSIC.

The complexity is of the order of 10^7 for MUSIC and 10^5 for Root MUSIC and *gold*-MUSIC under same system considerations. Fig. 8 indicates higher Order of Complexity and higher RMSE for Root MUSIC than *gold*-MUSIC. Therefore, *gold*-MUSIC provides better RMSE performance as compared with other two algorithms.

Table 8 exhibits trivial difference of estimated DOA from the actual DOA with varying ULA elements for different DOA estimators and DS-CDMA users. The estimated DOA improves as number of ULA elements increases. Additionally, *gold*-MUSIC is providing improved DOA estimate than MUSIC and Root MUSIC at SNR of 20 dB.

6. Conclusions

Evaluation of DOA estimation by *gold*-MUSIC is made feasible for ULA based DS-CDMA users with Propagation Delay diversity in Near-Far effect. The DOA estimated using *gold*-MUSIC shows clear and sharp peaks at the arriving angles with minimized sidelobes. Lesser RMSE of DOA estimation and enhanced computational efficiency is obtained for *gold*-MUSIC than that of with MUSIC and Root-MUSIC algorithms. The RMSE of DOA improves with increasing ULA elements, Data length and decreasing angle of arrival. Additionally, *gold*-MUSIC provides the detail spatial spectrum analogous to that with MUSIC. However, Root-MUSIC doesn't endow with that spatial spectrum.

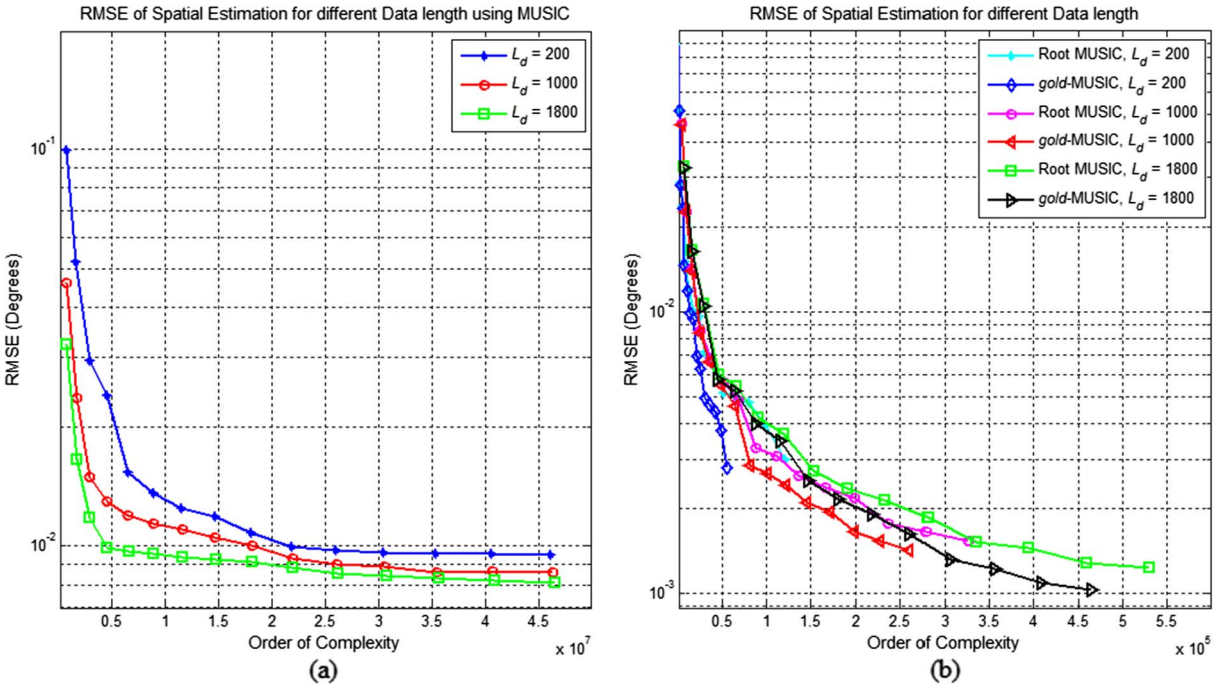

Fig. 8. Effect of User 1 Data length on variation of RMSE with Order of Complexity for Spatial Estimation algorithms: (a) MUSIC, (b) Root MUSIC and *gold*-MUSIC.

Table 8
Estimation of DOA for Case 3.

User	Measured DOA (Degrees) for SNR = 20 dB								
	2 element ULA			3 element ULA			4 element ULA		
	MUSIC	Root MUSIC	*gold*-MUSIC	MUSIC	Root MUSIC	*gold*-MUSIC	MUSIC	Root MUSIC	*gold*-MUSIC
User 1	19.959	19.979	19.983	19.969	19.987	19.993	19.974	19.992	19.999
User 2	−44.944	−44.966	−44.984	−44.956	−44.976	−44.993	−44.965	−44.987	−44.998
User 3	74.947	74.963	74.982	74.957	74.975	74.991	74.968	74.987	74.997

Appendix A. Supplementary material

Supplementary data associated with this article can be found, in the online version, at http://dx.doi.org/10.1016/j.aeue.2017.11.029.

References

[1] Zhang J, Zhang H, Cui Z. Dual-antenna-based blind joint hostile jamming cancellation and multi-user detection for uplink of asynchronous direct-sequence code-division multiple access systems. IET Commun 2013;7:911–21.
[2] Takeuchi K, Vehkaperä M, Tanaka T, Müller RR. Large-system analysis of joint channel and data estimation for MIMO DS-CDMA systems. IEEE Trans Inf Theory 2012;58:1385–412.
[3] Chung C, Chen W, Lin W. Realizable bandlimited DS-CDMA system occupying Nyquist bandwidth. IEEE Commun Lett 2012;16:964–7.
[4] Kusume K, Bauch G, Utschick W. IDMA vs. CDMA: analysis and comparison of two multiple access schemes. IEEE Trans Wireless Commun 2012;11:78–87.
[5] Gui G, Adachi F. Sparse least mean fourth algorithm for adaptive channel estimation in low signal-to-noise ratio region. Int J Commun Syst. John Wiley & Sons, Ltd. 2014;27:3147–57.
[6] Qing H, Liu Y, Xie G. Smart antenna-assisted spectrum sensing for robust detection in cognitive radio networks. Int J Commun Syst, John Wiley & Sons, Ltd 2016;29:2192–204.
[7] He J, Ahmad MO, Swamy MNS. Joint space-time parameter estimation for multi-carrier CDMA systems. IEEE Trans Veh Technol 2012;61:3306–11.
[8] Zhang Y, Lu L, Wang Y, Chen C. WLAN indoor localization method using angle estimation. Elsevier Int J Electron Commun (AEÜ) 2017;76:11–7.
[9] Olfat A, Nader-Esfahani S. New receiver for multiuser detection of CDMA signals with antenna arrays. IEE Proc – Commun 2004;151:143–51.
[10] Kutty S, Sen D. Beamforming for millimeter wave communications: an inclusive survey. IEEE Commun Surv Tutorials 2016;18:949–73.
[11] Cui K, Wu W, Huang J, Chen X, Yuan N. DOA estimation of LFM signals based on STFT and multiple invariance ESPRIT. Elsevier Int J Electron Commun (AEÜ) 2017;77:10–7.
[12] Chiang C, Chang A. DOA estimation in the asynchronous DS-CDMA system. IEEE Trans Antennas Propag 2003;AP-51:40–7.
[13] Rangarao KV, Venkatanarasimhan S. *gold*-MUSIC: a variation on MUSIC to accurately determine peaks of the spectrum. IEEE Trans Antennas Propag 2013;61:2263–8.
[14] Poormohammad S, Farzaneh F. Precision of direction of arrival (DOA) estimation using novel three dimensional array geometries. Elsevier Int J Electron Commun (AEÜ) 2017;75:35–45.
[15] Zekavat SA, Buehrar RM. Handbook of position location – theory, practice and advances. John Wiley & Sons, Inc. (published). IEEE Press, IEEE, Inc. (copyright); 2012.
[16] Mahnaz AP, Sedigheh G. M$\ell_{1,2}$-MUSIC algorithm for DOA estimation of coherent sources. IET Signal Proc 2017;11:429–36.
[17] Morabito AF, Laganà AR, Sorbello G, Isernia T. Mask-constrained power synthesis of maximally sparse linear arrays through a compressive-sensing-driven strategy. J Electromagn Waves Appl 2015;29:1384–96.
[18] Hosseini SMR, Sebt MA. Array interpolation using covariance matrix completion of minimum-size virtual array. IEEE Signal Process Lett 2017;24:1063–7.
[19] Berber SM. Noise-based spreading in code division multiple access systems for secure communications. Int J Commun Syst. John Wiley & Sons, Ltd. 2016;29:402–16.
[20] Dodd R, Schlegel C, Gaudet V. DS-CDMA implementation with iterative multiple access interference cancellation. IEEE Trans Circ Syst-I: Reg Pap 2013;60:222–31.
[21] Lathi BP, Ding Z. Modern digital and analog communication systems. International, 4th ed. New York: Oxford University Press, Inc.; 2010.
[22] Kuramoto ASR, Ciriaco F, Abrão T, Jeszensky PJE. Sequence design for MPG QS-CDMA systems based on heuristic combinatorial optimization. Wiley J Wireless Commun Mobile Comput 2012;12:236–47.

[23] Jensen JR, Christensen MG, Benesty J, Jensen SH. Joint spatio-temporal filtering methods for DOA and fundamental frequency estimation. IEEE/ACM Trans Audio Speech Lang Process 2015;23:174–85.
[24] Kaifas TN. Unconditional, on the directions of arrival, statistics of the adaptive antenna arrays. Wiley J Wireless Commun Mobile Comput 2013;13:1386–96.
[25] Song A, Wang A, Luan S, Qiu T. Widely linear generalized sidelobe canceling beamforming with variable diagonal loading. Elsevier Int J Electron Commun (AEÜ) 2017;76:77–85.
[26] Noh G, Bahng S, Park Y. BER minimization for dual-polarized wireless systems with polarization-domain rotation. Int J Commun Syst. John Wiley & Sons, Ltd. 2016;29:1128–37.
[27] Chen J, Ueng F. Adaptive antennas for MIMO OFDM-CDMA communication systems. Wiley J Wireless Commun Mobile Comput 2015;15:484–99.
[28] Durrani S, Bialkowski ME. Analysis of the error performance of adaptive array antennas for CDMA with noncoherent *M*-ary orthogonal modulation in Nakagami fading. IEEE Commun Lett 2005;9:148–50.
[29] Chinnadurai S, Selvaprabhu P, Jeong Y, Sarker AL, Hai H, Duan W, et al. User clustering and robust beamforming design in multicell MIMO-NOMA system for 5G communications. Elsevier Int J Electron Commun (AEÜ) 2017;78:181–91.
[30] Fan L, Zhang Y, Jiang Y, Fukawa K, Suzuki H, Wong K. Adaptive joint maximum-likelihood detection and minimum-mean-square error with successive interference canceler over spatially correlated multiple-input multiple-output channels. Wiley J Wireless Commun Mobile Comput 2013;13:1192–204.
[31] Li P, de Lamare RC. Adaptive decision-feedback detection with constellation constraints for MIMO systems. IEEE Trans Veh Technol 2012;61:853–9.
[32] Choi S, Yun D. Design of an adaptive antenna array for tracking the source of maximum power and its application to CDMA mobile communications. IEEE Trans Antennas Propag 1997;45:1393–404.
[33] Hilal HA. Neural networks applications for CDMA systems in non-Gaussian multipath channels. Elsevier Int J Electron Commun (AEÜ) 2017;73:150–6.
[34] Brent R. Algorithms for minimization without derivatives. Englewood Cliffs, NJ, USA: Prentice-Hall; 1973.
[35] Cao Y, Zhang Z, Dai F, Xie R. Direction of arrival estimation for monostatic multiple-input multiple-output radar with arbitrary array structures. IET Radar Sonar Navig 2012;6:679–86.
[36] Rübsamen M, Gershman AB. Direction-of-arrival estimation for nonuniform sensor arrays: from manifold separation to Fourier domain MUSIC methods. IEEE Trans Signal Process 2009;57:588–99.